Heterobi- to heterotetrametallic transition metal complexes constructed from ferrocenecarboxylate and [{[Ti](μ-σ,π-C≡CSiMe₃)₂}M]⁺ units

Janett Kühnert [a], Martin Lamač [b], Tobias Rüffer [a], Bernhard Walfort [a], Petr Štěpnička [b], Heinrich Lang [a,*]

[a] *Technische Universität Chemnitz, Fakultät für Naturwissenschaften, Institut für Chemie, Lehrstuhl für Anorganische Chemie, Straße der Nationen 62, 09111 Chemnitz, Germany*
[b] *Charles University, Faculty of Science, Department of Inorganic Chemistry, Hlavova 2030, 12840 Prague 2, Czech Republic*

Abstract

A series of copper(I) and silver(I) carboxylates received from various ferrocenecarboxylic acids was synthesized and used in the preparation of heterooligometallic Ti–Cu(Ag)–Fe complexes. The silver(I) salts [FcCO₂Ag] (**2a**) and [FcCH=CHCO₂Ag] (**2b**) (Fc = ferrocenyl, $(\eta^5\text{-}C_5H_4)Fe(\eta^5\text{-}C_5H_5)$) were obtained through deprotonation of the respective acids FcCO₂H (**1a**) and FcCH=CHCO₂H (**1b**) with NEt₃, followed by a reaction with [AgNO₃]. The heterotrimetallic complexes {[Ti](μ-σ,π-C≡CSiMe₃)₂}AgO₂CFc (**4a**) and {[Ti](μ-σ, π-C≡CSiMe₃)₂}AgO₂CCH=CHFc (**4b**), where [Ti] denotes the $(\eta^5\text{-}C_5H_4SiMe_3)_2Ti$ unit, were obtained from the reaction of **2a** and **2b** with the organometallic π-tweezer compound [Ti](C≡CSiMe₃)₂ (**3**). The related heterotrimetallic copper(I) complex {[Ti](μ-σ, π-C≡CSiMe₃)₂}CuO₂CFc (**9a**) was prepared via two synthetic routes. First, salt **2a** was reacted with $[(\eta^2\text{-}Me_3SiC\equiv CSiMe_3)CuBr]_2$ (**10**) to give the alkyne-stabilized copper(I) carboxylate $[(\eta^2\text{-}Me_3SiC\equiv CSiMe_3)(CuO_2CFc)_2]_2$ (**11**). Subsequent reaction of **11** with four equivalents of **3** afforded **9a**. Alternatively, **9a** and its analogues {[Ti](μ-σ,π-C≡CSiMe₃)₂}CuO₂C–E–Fc (E = *trans*-CH=CH (**9b**), CH₂CH₂ (**9c**)), were prepared from acidolysis of the Cu–C_Me bond in {[Ti](μ-σ,π-C≡CSiMe₃)₂}CuMe (**8**) with acids **1a**–**1c**. An analogous reaction between HO₂CfcPPh₂M(CO)₅ (M = Cr (**14a**), Mo (**14b**), W (**14c**); fc = ferrocene-1,1′-diyl) and **8** at −30 °C gave the alkyne/ferrocene-bridged heterotetrametallic compounds {[Ti](μ-σ,π-C≡CSiMe₃)₂}CuO₂CfcPPh₂M(CO)₅ (M = Cr (**15a**), Mo (**15b**), W (**15c**)). Reversing the reaction steps so that {[Ti](μ-σ,π-C≡CSiMe₃)₂}CuO₂CfcPPh₂ (**12**) was prepared first and then reacted with M(CO)₅(thf) (M = Cr (**13a**), Mo (**13b**), W (**13a**)) gave complicated reaction mixtures from which pure **15a**–**15c** could not be isolated. The solid-state structures of **5**, **7**, **9a**, and **11** have been corroborated by single-crystal X-ray structural studies and the electrochemical behavior of acids **1a**–**1c** and of complexes **4a**, **4b** and **9a**–**9c** was studied by cyclic voltammetry.
© 2007 Elsevier B.V. All rights reserved.

Keywords: Ferrocenecarboxylic acids; Organometallic π-tweezers; Titanium; Silver; Copper; Group-6 metal carbonyls; X-ray structure; Cyclic voltammetry

1. Introduction

The concept of molecular "tinkertoys" described by Michl and co-workers [1], or "Lego®" approach introduced [2] and developed by Raymo and Stoddart [3] includes the construction of large complex molecules by connecting independent building blocks. Prerequisites of the successful application of this approach are the availability of suitable structural fragments and synthetic methods for their assembly. Recently, it has been shown that this approach can also be applied toward the preparation of heteromultinuclear transition metal complexes [4]. Compounds thus prepared offer the possibility to study

---

electronic communication between different redox-active metal atoms in oligometallic molecules and may act as catalytically active systems for homogeneous catalysis, providing cooperative effects due to the presence of additional metal centers [5].

We report here about the synthesis of copper(I) and silver(I) carboxylates with several ferrocenecarboxylic acids and their use in the preparation of heterooligometallic complexes with organometallic π-tweezer precursors. Furthermore, in the case of 1′-(diphenylphosphanyl)-1-ferrocenecarboxylic acid (Hdpf) [6], we made use of the coordination ability of the phosphanyl group toward different transition metal fragments to synthesize complexes of higher nuclearity. The advantage of the ferrocene backbone is seen not only in its synthetic versatility and robustness, but also as a redox probe. The observed electrochemical properties of the resulting heterodi-, -triand -tetrametallic complexes are discussed as well.

2. Results and discussion

2.1. Syntheses and characterization of Ag(I) complexes

Heterotrimetallic Ti–Ag–Fe complexes of type {[Ti]-(μ-σ,π-C≡CSiMe$_3$)$_2$}AgO$_2$CFc (**4a**) and {[Ti](μ-σ, π-C≡CSiMe$_3$)$_2$}AgO$_2$CCH=CHFc (**4b**) (Fc = ferrocenyl, fc = ferrocene-1,1′-diyl) are accessible in a two-step procedure from FcCO$_2$H (**1a**) and FcCH=CHCO$_2$H (**1b**), respectively, as outlined in Scheme 1. The starting silver(I) salts [FcCO$_2$Ag] (**2a**) and [FcCH=CHCO$_2$Ag] (**2b**) were prepared by the reaction of the respective ferrocene carboxylic acids, FcCO$_2$H (**1a**) and FcCH=CHCO$_2$H (**1b**), with [AgNO$_3$] in the presence of triethylamine in ethanol at 25 °C [7]. However, attempts to prepare the analogous silver(I) system from 3-ferrocenylpropionic acid (FcCH$_2$-CH$_2$CO$_2$H, **1c**) under similar reaction conditions failed. On addition of FcCH$_2$CH$_2$CO$_2^-$NEt$_3$H$^+$ to a [AgNO$_3$]-containing ethanol solution the color immediately changed to green indicating that most likely the ferrocene moiety was oxidized. None the less, the appropriate ferrocenium system could not be isolated, due to rapid decomposition. This different behavior results from a higher electron density at iron which makes the Fc unit easier to oxidize (for comparison see Table 2).

Complexes **4a** and **4b** resulted from combining the respective silver salts **2a** and **2b** with the organometallic π-tweezer [Ti](C≡CSiMe$_3$)$_2$ (**3**; [Ti] = (η^5-C$_5$H$_4$SiMe$_3$)$_2$Ti) at the molar ratio of 1:1 in tetrahydrofuran at 25 °C.
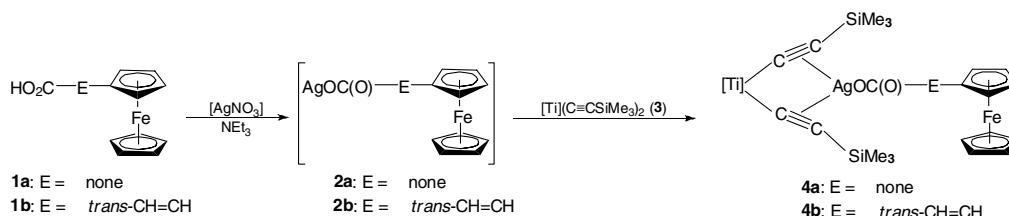
Whereas heterotrimetallic **4a** and **4b** dissolve well in common organic solvents the silver(I) salts **2a** and **2b** are practically insoluble. Hence, the silver(I) salts could be characterized only by elemental analysis and IR spectroscopy. The more soluble complexes **4a** and **4b** have been characterized similarly and also by multinuclear NMR spectroscopy. IR spectra of **4a** and **4b** show the characteristic C≡C stretching vibrations of the Ti–C≡C–Si units which are observed at 1948 (**4a**) and 1942 cm^{-1} (**4b**), respectively, which are shifted to lower wave-numbers as compared with free **3** [8]. Similar observations have been made for titanium–silver heterobimetallic π-tweezers, such as {[Ti](μ-σ,π-C≡CSiMe$_3$)$_2$}AgOSO$_2$CF$_3$ [8].

The NMR properties of these compounds correspond with their formulated structures. The ^{1}H NMR spectra of **4a**–**4b** are in accordance with the proposed formulation, displaying signals due to the titanocene tweezer and the ferrocene moieties. In ^{13}C{^{1}H} NMR spectra, the alkynyl carbon atoms C$_\alpha$ and C$_\beta$ give rise to doublets due to coupling with the embedded silver(I) ion (**4a**: C$_\alpha$: δ_C 155.4, J_{AgC} = 15 Hz; C$_\beta$: δ_C 138.3, J_{AgC} = 6 Hz; **4b**: C$_\alpha$: δ_C 156.0, J_{AgC} = 15 Hz; C$_\beta$: δ_C 137.4, J_{AgC} = 7 Hz). Any further splitting resulting from the occurrence of isotopomers containing the silver isotopes ^{107}Ag and ^{109}Ag (both I = 1/2, ^{107}Ag 51.8%, ^{109}Ag 48.2%) [9] is not observed. Likewise, the ^{29}Si{^{1}H} NMR spectra of **4a** and **4b** show coupling for the C≡CSiMe$_3$ silicon atoms with the silver(I) ions (J_{AgSi} = 2 Hz).

Next we used the hybrid ferrocene phosphanylcarboxylic acid Hdpf [6] as a starting material for the synthesis of complexes of higher nuclearity as it offers the possibility of extending the ferrocene-bridged assemblies via coordination of its phosphanyl functionality. Deprotonation of Hdpf with triethylamine and reaction with [AgNO$_3$] in ethanol leads to the tetrameric silver(I) salt [Ag(dpf)]$_4$ (**5**). Unfortunately, all attempts to react **5** with the π-tweezer molecule **3** to give **6** have been unsuccessful (Scheme 2); only a mixture of *non*-separable products was obtained. Using a diethyl ether–ethanol mixture of 6:1 as a solvent in the reaction of Hdpf with NEt$_3$/[AgNO$_3$] instead of pure ethanol leads to [Ag(dpf)(Hdpf)] (**7**) (Scheme 2), probably because of incomplete deprotonation of the carboxyl function by triethylamine in the mixed solvent.

The NMR spectral properties of **5** and **7** correlate with their formulated structures. In the ^{1}H NMR of **5** and **7** the cyclopentadienyl protons give rise to four signals between δ_H 4.04 and 4.85, the pattern being slightly different for the two compounds. The ^{13}C{^{1}H} NMR signal of the carbonyl carbon is found at δ_C 171.8 for **5** and at δ_C

Scheme 1. Synthesis of **4a** and **4b**.
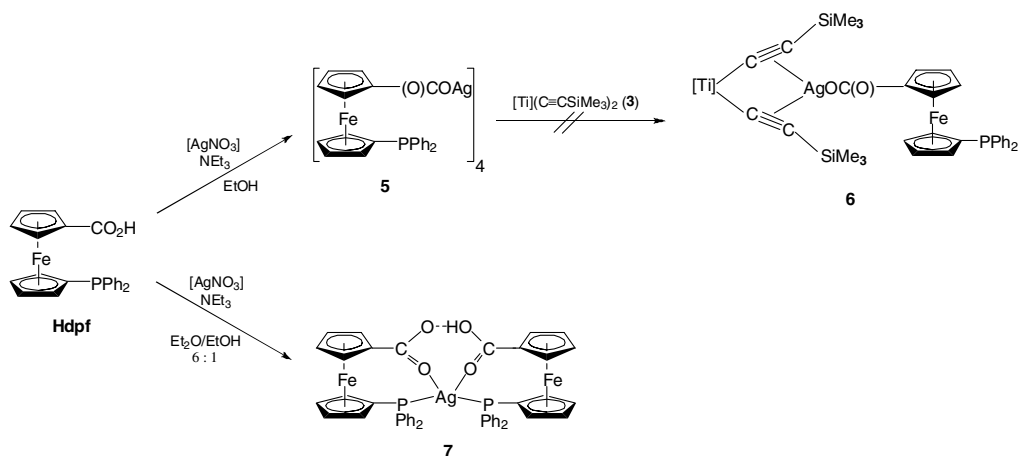
Scheme 2. Synthesis of compounds **5** and **7** from Hdpf and [AgNO$_3$], respectively.

178.2 for **7**. The ^{31}P{^{1}H} NMR signals of **5** and **7** are split into a pair of doublets due to the presence of the silver isotopes ^{107}Ag and ^{109}Ag (vide supra). Complex **5** resonates at δ_P 5.1 with $^1J_{109Ag31P} = 790$ Hz and $^1J_{107Ag31P} = 669$ Hz, while the signal of **7** occurs at δ_P −1.8 with coupling constants $^1J_{109Ag31P} = 526$ Hz and $^1J_{107Ag31P} = 456$ Hz. This difference can be attributed to the different structures of the complexes.

2.2. Syntheses and characterization of Cu(I) complexes

Trimetallic Ti–Cu–Fe complexes of structural type {[Ti](μ-σ,π-C≡CSiMe$_3$)$_2$}CuO$_2$C–E–Fc (E = none (**9a**), *trans*-CH=CH (**9b**), and CH$_2$CH$_2$ (**9c**)) were obtained from the reaction of {[Ti](μ-σ,π-C≡CSiMe$_3$)$_2$}CuMe (**8**) with the appropriate acid in equimolar amounts at −30 °C. The reaction proceeds under H$^+$ transfer and loss of CH$_4$ to afford the heterotrimetallic complexes **9a**–**9c** in virtually quantitative yields (Eq. (1)).

(1)
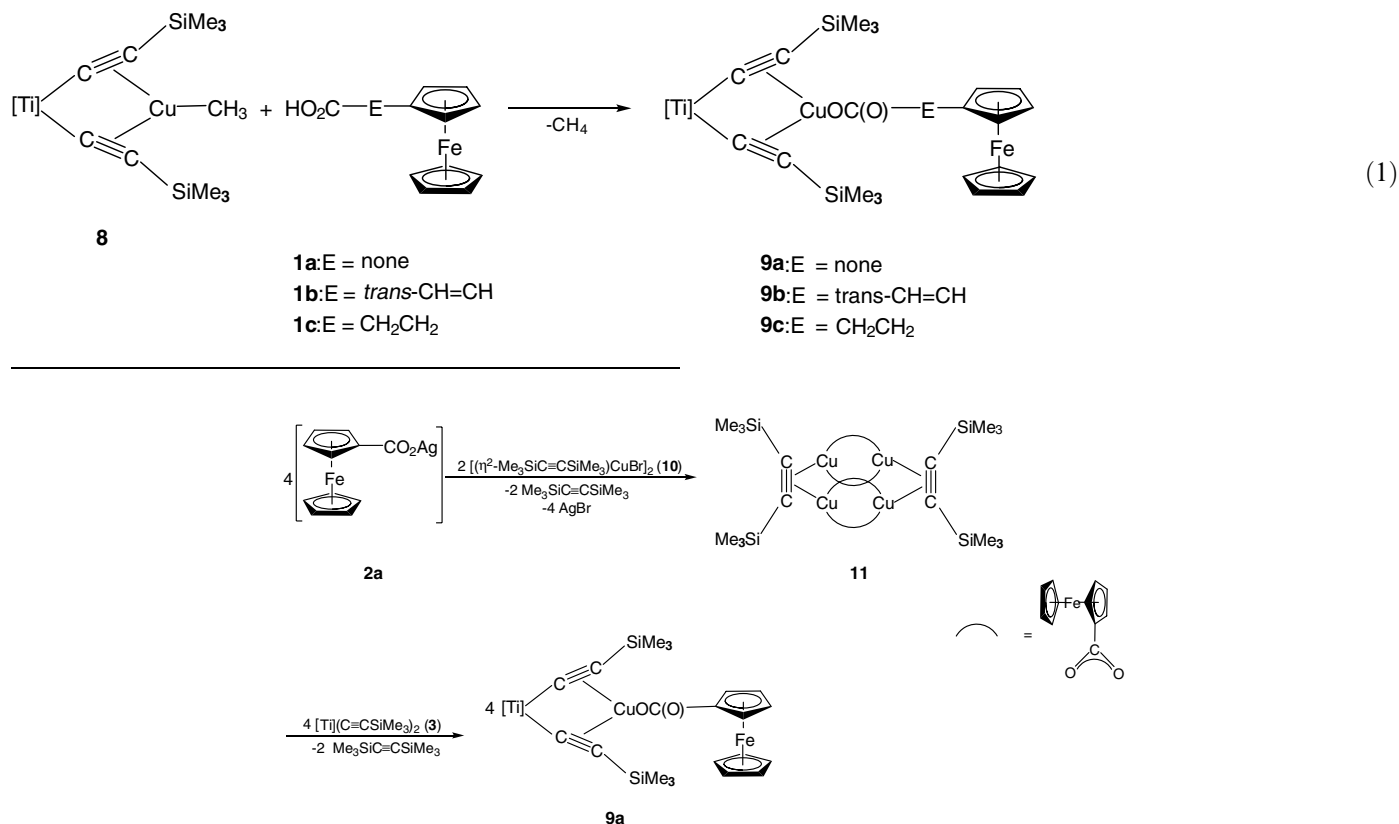
Scheme 3. Synthesis of **9a** via copper(I) carboxylate **11**.
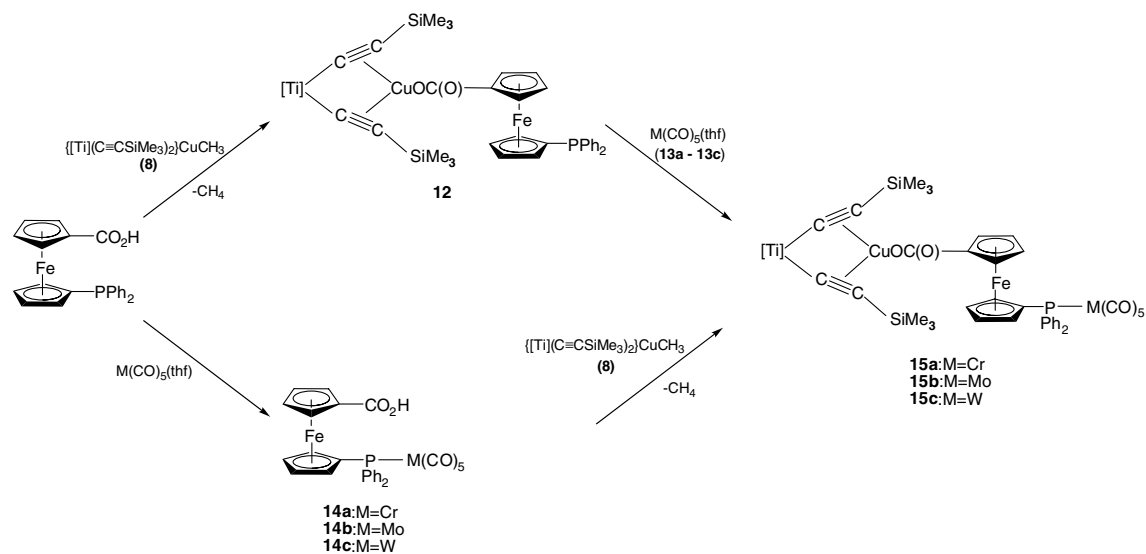
Scheme 4. Synthesis of heterotetrametallic complexes **15a**–**15c**.

An alternative synthesis procedure leading to **9a** is outlined in Scheme 3. The silver(I) salt **2a** is treated first with the dicopper(I) complex $[(\eta^2\text{-Me}_3SiC{\equiv}CSiMe_3)CuBr]_2$ (**10**) [8b] at the molar ratio of 2:1 in tetrahydrofuran at 0 °C to give the tetranuclear alkyne-stabilized copper(I) carboxylate $[(\eta^2\text{-Me}_3SiC{\equiv}CSiMe_3)(CuO_2CFc)_2]_2$ (**11**). In a subsequent reaction with four equivalents of the π-tweezer **3**, compound **11** gives the Ti–Cu–Fe molecule **9a** as an orange solid in 87% yield after appropriate work-up.

Reacting Hdpf with **8** under reaction conditions similar to the synthesis of **9a**–**9c** (vide supra) gave heterotrimetallic $\{[Ti](\mu\text{-}\sigma,\pi\text{-}C{\equiv}CSiMe_3)_2\}CuO_2CfcPPh_2$ (**12**) which possesses a terminal phosphane group (Scheme 4). Unfortunately, compound **12** is rather unstable, especially in solution. It becomes very easily oxidized at the phosphorus atom very likely because the presence of the π-tweezer moiety increases the electron density at the PPh$_2$ group. Treatment of **12** with equimolar amounts of M(CO)$_5$(thf) (M = Cr (**13a**), Mo (**13b**), W (**13c**)) [10] gave only small amounts of the desired Ti–Cu–Fe–M complexes **15a**–**15c** (Scheme 4) that could not be isolated in pure form either by crystallization or column chromatography from the obtained reaction mixtures. On the other hand, reacting pre-formed HdpfM(CO)$_5$ (M = Cr (**14a**), Mo (**14b**), W (**14c**)) [11] with **8** in a 1:1 molar ratio gave the expected heterotetrametallic complexes $\{[Ti](\mu\text{-}\sigma,\pi\text{-}C{\equiv}CSiMe_3)_2\}$-CuO$_2$CfcPPh$_2$M(CO)$_5$ (M = Cr (**15a**), Mo (**15b**), W (**15c**); Scheme 4). However, owing to the considerable instability of **15a**–**15c**, even in solid state, only **15b** could be isolated in purity sufficient for spectroscopically characterization.

In an attempt to prepare a Ti–Cu–Fe–Ru compound with the free phosphorus atom in **12** coordinating to Ru(η^6-1,4-MeC$_6$H$_4$(CHMe$_2$))Cl$_2$ we reacted [RuCl$_2$(η^6-1,4-MeC$_6$H$_4$(CHMe$_2$))]$_2$ [12] with **12** and, alternatively, also **8** with RuCl$_2$(Hdpf)(η^6-1,4-MeC$_6$H$_4$(CHMe$_2$)) [13].

In both cases the work-up gave exclusively the known CuCl-tweezer complex $\{[Ti](\mu\text{-}\sigma,\pi\text{-}C{\equiv}CSiMe_3)_2\}CuCl$ (**16**) [8]. The product **16** resulting via chloride transfer from the ruthenium dichloride species to copper is apparently thermodynamically more stable than the anticipated heterotetrametallic complex. The observed reaction behavior parallels that reported for the reaction between, i.e. [Ti](C≡C-1-C$_6$H$_4$-4-C≡N-4)$_2$ and various [CuX] sources (X = Cl, I), where only heterobimetallic π-tweezer complexes $\{[Ti](\mu\text{-}\sigma,\pi\text{-}C{\equiv}CC_6H_4C{\equiv}N\text{-}4)_2\}CuX$ have been isolated [14].

Complexes **9a**–**9c**, **11**, and **12** were characterized by elemental analysis, IR and NMR spectroscopy. Unfortunately, due to the instability of **15a**–**15c**, even in the solid state, it was possible to record complete NMR data only for **15b**. All complexes show C≡C stretching vibrations at ca. 1915 cm^{-1}. The NMR spectroscopic properties of these copper(I) complexes confirm their proposed structures. In the ^{1}H NMR spectra of all copper(I) compounds, the signals due to the ferrocene cyclopentadienyls are observed in the range from δ_P 4.00 to 4.66. The signals of the Me$_3$Si groups are found as one or two singlets in the range δ_P 0.20–0.26 (**9a**–**9c**, **12**, **15b**) or at δ_P 0.43 (**11**). In the ^{13}C{^{1}H} NMR spectra of **15b** one doublet is observed for the equatorial CO ligands at δ_C 206.0 Hz ($^2J_{PC}$ = 9 Hz). However, the signal for the axial CO could not be detected. The product resulting by complexation of Hdpf with the π-tweezer molecule **8** did not exert a significant ^{31}P{^{1}H} NMR coordination shift (cf. δ_P −19.1 for Hdpf and −17.9 for **12**). Nevertheless, when M(CO)$_5$ units are introduced as in **15a**–**15c**, a remarkable shift is observed (cf. δ_P −17.9 (**12**) to 45.6 (**15a**), 26.7 (**15b**), and 9.5 (**15c**)), corresponding to δ_P values reported for the series of (Hdpf)M(CO)$_5$ complexes (cf. δ_P 46.0 (Cr), 26.6 (Mo), and 9.3 (W)) [11].

2.3. X-ray structure analysis

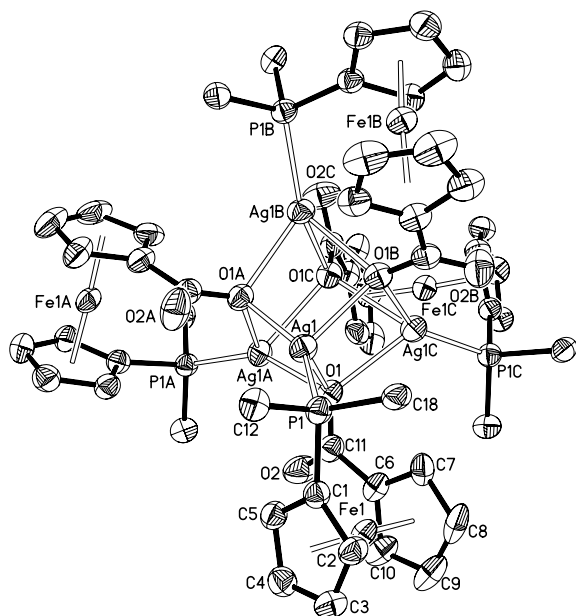The solid state structures of **5** (Figs. 1 and 2), **7** (Fig. 3), **9a** (Fig. 4), and **11** (Fig. 5) were established by single-crys-tal X-ray structure analysis. Relevant crystallographic and structure refinement data are summarized in Table 3.

Complex **5** crystallizes in the tetragonal space-group $P4_2/n$. Its tetrameric nature gives rise to a highly symmetric though distorted heterocubane core Ag_4O_4 (Fig. 2) symmetrically surrounded by the bidentated ferrocene phosphanyl-carboxylato moieties (Fig. 1). A distorted tetrahedral coordination geometry is built around each silver ion by one phosphorus and three oxygen atoms (P1–Ag1–O1B,

Fig. 1. ORTEP plot (50% probability level) of **5** with the atom numbering scheme (the hydrogen atoms, two *non*-coordinating CH_2Cl_2 molecules and the phenyl ring carbons are omitted for clarity). Atoms generated by the crystallographic symmetry operations $(-x + 1/2, -y + 1/2, z)$ (A), $(y, -x + 1/2, -z + 1/2)$ (B), $(-y + 1/2, x, -z + 1/2)$ (C) are distinguished with the suffixes A, B, and C. Selected bond distances (Å) and angles (°): C11–O1, 1.290(6); C11–O2, 1.226(6); Ag1–P1, 2.3501(12); Ag1–O1, 2.535(3); Ag1–O1A, 2.291(3); Ag1–O1B, 2.448(3); Ag1A–O1, 2.291(3); Ag1C–O1, 2.448(3); Fe1–D1, 1.643(2); Fe1–D2, 1.656(2); O1A–Ag1–P1, 149.98(9); O1A–Ag1–O1B, 82.10(12); P1–Ag1–O1B, 123.96(8); O1A–Ag1–O1, 77.93(11); P–Ag1–O1, 119.15(8); O1B–Ag1–O1, 73.33(11); (D1 = centroid of $C_5H_4PPh_2$, D2 = centroid of $C_5H_4CO_2$).

Fig. 3. ORTEP plot (50% probability level) of **7** with the atom numbering scheme (the hydrogen atoms (except H2A) and one *non*-coordinating CH_2Cl_2 molecule are omitted for clarity). Atoms generated by the crystallographic $(-x + 4, -y + 2, z)$ symmetry operation are distinguished with the suffix A. Selected bond distances (Å) and angles (°): Ag1–O1, 2.4258(16); Ag1–O1A, 2.4258(16); Ag1–P1, 2.4283(5); Ag1–P1A, 2.4283(5); C23–O1, 1.238(3); C23–O2, 1.288(3); O2–O2A, 2.449(3); Fe1–D1, 1.6512(14); Fe2–D2, 1.6518(13) (D1 = centroid of $C_5H_4CO_2$, D2 = centroid of $C_5H_4PPh_2$); O1A–Ag1–O1, 79.69(9); O1A–Ag1–P1, 106.60(4); O1–Ag1–P1A, 106.60(4); O1A–Ag1–P1A, 107.41(4); O1–Ag1–P1, 107.41(4); P1A–Ag1–P1, 135.21 (3); C23–O1–Ag1, 121.33(15); O1–C23–O2, 124.3(2).
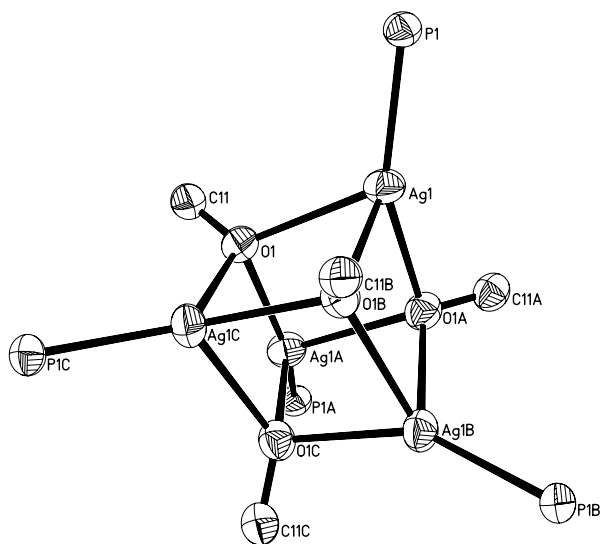

Fig. 2. A view of the silver–oxygen heterocubane core in complex **5**. Displacement ellipsoids correspond to 50% probability.
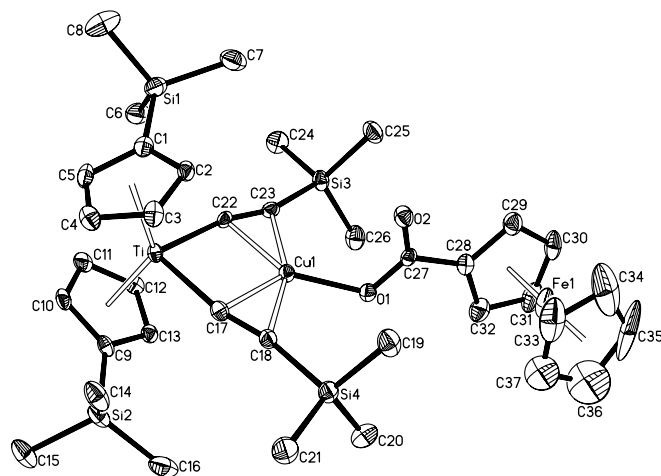

Fig. 4. ORTEP diagram (30% probability level) of **9a** with the atom numbering scheme (the hydrogen atoms are omitted for clarity).
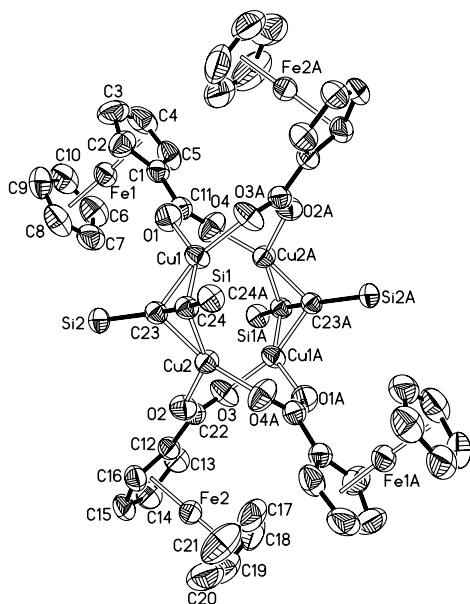
Fig. 5. ORTEP diagram (50% probability) of **11** with the atom numbering scheme (hydrogen atoms and methyl groups are omitted for clarity). Symmetry generated atoms are named with the suffix A and generated by the $(-x + 1, -y + 2, -z + 1)$ operation. Selected bond distances (Å) and angles (°): C23–C24, 1.274(2); C22–O2, 1.252(2); C22–O3, 1.246(2); C11–O1, 1.250(2); C11–O4, 1.247(2); Cu1–C23, 2.0033(18); Cu1–C24, 1.9972(19); Cu2–C23, 1.9941(18); Cu2–C24, 1.9880(17); Fe1–D1, 1.6503(12); Fe1–D2, 1.6571(13); Fe1–D3, 1.6394(12); Fe1–D4, 1.641(2); Cu1–O1, 1.9414(15); Cu1–O3A, 1.9491(15); Cu2–O2, 1.9531(13); Cu2–O4A, 1.9388(15); Cu1–Cu2, 2.9770(10); Cu1–Cu2A, 3.0754(11); Si1–C23–C24, 160.56(16); Si2–C24–C23, 157.74(16); O1–Cu1–O3A, 102.62(7); O1–Cu1–C24, 145.72(7); O1–Cu1–C23, 111.84(7); O3A–Cu1–C23, 142.64(7), C24–Cu1–C23, 37.14(7); C24–Cu2–C23, 37.32(7). Definitions: D1, D3 = centroids of C_5H_4, D2, D4 = centroids of C_5H_5.

Table 1
A comparison of bond distances (Å) and angles (°) in symmetrically independent molecules of **9a**

9aA (with Cu1)		**9aB** (with Cu2)	
Bond distances (Å)			
Fe1–D1[a]	1.633(3)	Fe2–D3	1.635(3)
Fe1–D2	1.661(6)	Fe2–D4	1.656(6)
C27–O1	1.269(7)	C64–O3	1.278(7)
C27–O2	1.242(7)	C64–O4	1.235(6)
Cu1–O1	1.936(4)	Cu2–O3	1.927(4)
Cu1–C17	2.070(6)	Cu2–C59	2.072(6)
Cu1–C18	2.128(6)	Cu2–C60	2.117(6)
Cu1–C22	2.074(6)	Cu2–C54	2.071(6)
Cu1–C23	2.133(6)	Cu2–C55	2.126(6)
C17–C18	1.237(8)	C59–C60	1.242(8)
C22–C23	1.240(8)	C54–C55	1.241(8)
Ti1–C17	2.108(6)	Ti2–C59	2.100(6)
Ti1–C22	2.093(6)	Ti2–C54	2.091(6)
Ti1–D5	2.041(4)	Ti2–D7	2.042(4)
Ti1–D6	2.043(3)	Ti2–D8	2.042(3)
C23–Si3	1.867(6)	Cu1–Ti	2.9644(13)
C18–Si4	1.850(7)		
Bond angles (°)			
Ti1–C17–C18	165.8(5)	Ti2–C59–C60	165.4(5)
Ti1–C22–C23	166.1(5)	Ti2–C54–C55	166.1(5)
C17–C18–Si4	165.3(5)	C59–C60–Si8	164.7(5)
C22–C23–Si3	161.1(5)	C54–C55–Si7	160.7(5)
C27–O1–Cu1	117.1(4)	C64–O3–Cu2	117.1(4)
C17–Ti1–C22	88.7(2)	C59–Ti2–C54	88.6(2)
C17–C18–Si4	165.3(5)	C22–C23–Si3	161.1(5)

[a] D1, D3 = centroids of $C_5H_4CO_2$; D2, D4 = centroids of C_5H_5; D5, D6, D7, D8 = centroids of the $C_5H_4SiMe_3$ units.

123.96(8)°; O1A–Ag1–O1, 77.93(11)°; P1–Ag1–O1B, 123.96(8)°. The oxygen atoms within the cube are part of the carboxyl function attached to the ferrocene units, acting as μ_3-bridges (C11–O2, 1.226(6); C11–O1, 1.290(6) Å). Each O–Ag edge is spanned by the ferrocene moiety so that the phosphanylcarboxylate donor binds to the silver(I) ion via its phosphorus atom (Ag1–P1, 2.3501(12) Å). The ferrocene cyclopentadienyl rings are rotated by ca. 4° to each other which represents an almost eclipsed conformation and show a tilting of only 3.1(3)°.

Orange crystals of **7** were obtained from a concentrated dichloromethane solution at 0 °C. Complex **7** crystallizes in the tetrahedral space group $I4_1$, mimicking a twofold symmetry. The silver atom Ag1 is σ-bonded to one oxygen atom from both carboxyl functions and coordinated by both phosphorus atoms (Ag1–O1, 2.4258(16); Ag1–P1, 2.4283(5) Å). The hydroxyl group of the protonated carboxyl function (C23–O1, 1.238(3); C23–O2, 1.288(3) Å) forms a hydrogen bridge to the carboxylate group (O2···O2A, 2.449(3) Å) which stabilizes the structure. Due to the overall symmetry, the H2A atom is disordered over two positions (as if bonded to O2 or O2A) with occupancies fixed at 0.5. The tetrahedral environment around the silver atom built from two oxygen and two phosphorus

atoms show some angular deformation attributable to steric congestion at the edge accommodating the bulky phosphane units (O1A–Ag1–O1, 79.69(9)°; O1A–Ag1–P1, 106.60(4)°; O1–Ag1–P1A, 106.60(4)°; O1A–Ag1–P1A, 107.41(4)°; O1–Ag1–P1, 107.41(4)°; P1A–Ag1–P1, 135.21(3)°). In contrast to **5** the tilting of the cyclopentadienyl rings is 2.59(18)° and they are rotated 12.7° to each other.

Heterotrimetallic **9a** crystallizes in the triclinic spacegroup $P\bar{1}$ with two independent molecules **9aA** (with Cu1) and **9aB** (with Cu2) in the asymmetric unit. The view of the molecular solid-state structure of **9aA** is shown in Fig. 4. The individual molecules are very similar in bond lengths and angles as well as in the overall molecular conformation (see Table 1).

In heterotrimetallic complex **9a** the Cu1 is σ-bonded to O1 (cf. Cu1–O1, 1.936(4) Å for **9aA**) from the carboxylic function and further surrounded by two η^2-coordinating Ti–C≡C–Si groups. All structural features of the organometallic π-tweezer ligand are in accordance most common to this type of early-late Ti–Cu complexes [8a,15]. The cyclopentadienyl rings of the ferrocene moiety are rotated by 24° in **9aA** and by 21° in **9aB** and show a tilting of the cyclopentadienyl rings of 2.1(6)° in **9aA** and 2.7(7)° in **9aB**. These differences, however, are attributable to packaging effects.

Yellow crystals of **11** resulted from a slow diffusion of *n*-pentane into a dichloromethane solution containing **11** at

25 °C. The compound crystallized as a *non*-stoichiometric solvate with the solvent molecules disordered in structural voids. The structural determination of **11** was rather complicated, since some residual peaks occurred in the electron density difference map. They correspond to solvent molecules present in the crystals. The peaks could not be attributed to ordered molecules and it was judged preferable to omit them from calculations by the use of the SQUEEZE procedure in PLATON-94 [16,17]. However, from ^{1}H NMR studies of single crystals of **11** it could be shown that dichloromethane and *n*-pentane are present in the crystalline material.

Complex **11** crystallizes in the triclinic space group $P\bar{1}$. A main characteristic feature of **11** is the paddle wheel-like, tetrameric arrangement of the four ferrocenyl moieties. Two ferrocenecarboxylate building blocks form bridges between a pair of copper(I) ions. The $(FcCO_2)_2Cu_2$ units thus formed are interconnected via a μ-η^2:η^2-coordinated alkyne into a symmetric tetramer showing Cu···Cu separations of 2.9770(10) (Cu1···Cu2) and 3.0754(11) Å (Cu1···Cu2A) (Cu1–C23, 2.0033(18); Cu1–C24, 1.9972(19); Cu2–C23, 1.9941(18); Cu2–C24, 1.9880(17) Å). In contrast to $[(\eta^2$-Me$_3$SiC≡CSiMe$_3$)(CuO$_2$CH$_3$)$_2]_2$ [18], the Cu···Cu distances in **11** mutually differ by ca. 0.1 Å. However, other structural features of the Cu–alkynyl unit are very similar to those of the related (η^2-alkyne)copper(I) complexes [19]. The cyclopentadienyl rings of the ferrocenyl moieties are rotated by ca. 17° (Fe1) or 10° (Fe2) and show tilts of 2.89(15)° (Fe1) and 2.6(2)° (Fe2). The Fe1 atom exhibits separations of 1.6503(12) and 1.6571(13) Å to the ring centroids D1 and D2, while 1.6394(12) and 1.641(2) Å are found for Fe2 and centroids D3 and D4, respectively (D1, D3 = centroids of the substituted cyclopentadienyl ring C$_5$H$_4$, D2, D4 = centroids of the cyclopentadienyl ring C$_5$H$_5$).

2.4. Electrochemistry

The series involving heterotrimetallic complexes **4a**–**b**, **9a**–**9c**, the organometallic π-tweezer **3**, and their parent

acids **1a**–**1c** was studied by cyclic voltammetry at a platinum electrode in dichloromethane solutions (see Section 4 for more details). Pertinent electrochemical data are summarized in Table 2; all potentials are given relative to that of the ferrocene/ferrocenium couple [20].

As expected, acids **1a**–**1c** undergo reversible one-electron oxidation of the ferrocene moiety to the corresponding ferrocenium. Redox potential of the ferrocene/ferrocenium couple decreases in the order **1a** > **1b** > **1c**, clearly reflecting the properties of the linker between the ferrocene unit and the carboxyl group. The presence of a two-carbon spacer group in **1b** and **1c** reduces the influence of the carboxyl group (i) via increasing its distance of the ferrocene unit and (ii) via compensating its electron-withdrawing influence by own electronic-donor and electron-relay properties. Consequently, the acid **1c** possessing the saturated bridge as the strongest electron donor and *non*-conjugated insulating bridge is oxidized most easily, i.e. at lowest potentials. In addition, the acids show broad, ill-defined reduction waves between −1.47 and −1.61 V attributable to the reduction of their carboxyl groups. The redox behavior of tweezer **3** is also rather simple as the compound undergoes a single reversible reduction at −1.72 V [8,21]. The wave is attributable to the reversible reduction of the Ti(IV) titanocene fragment and appears shifted by 90 mV positively as compared with the value obtained in an acetonitrile solution [21].

The redox response of the trimetallic complexes is much more complex, allowing only for a semiqualitative discussion. Thus, **4b** undergoes reversible oxidation of the ferrocene moiety at 0.02 V, which is 160 mV more negative than the redox process of **1b**. The cathodic region of the cyclic voltammogram shows an irreversible reduction wave at −1.53 V and a reduction at −1.86 V (Table 2) that are attributable to silver- and titanocene-centered reductions, respectively. The reduction behavior of the *non*-spaced analogue **4a** is quite similar, though with the respective waves occurring at −1.48 and ca. −1.81 V. The reduction potential of the process $T(IV) + e^- \rightarrow Ti(III)$ is almost independent of the chemical identity of the central ions in the heterometallic complexes. They agree with the free organometallic π-tweezer ligand. This is in agreement with the suggested fragmentation occurring as a consequence after reduction of the silver(I) or copper(I) (see below) metal ions resulting in the same bis(alkynyl) titanocene system in all cases [21]. In the anodic region, compound **4a** shows two oxidation waves: a reversible one at 0.00 V, due to the ferrocene/ferrocenium couple followed by a broad and smaller though reversible wave at ca. 0.26 V (Table 2).

The parallel series of copper(I) organometallic π-tweezer complexes shows similar differences between the **1a**-based compound **9a** on one hand and the 'spaced' complexes **9b** and **9c** on the other. Compound **9a** is oxidized in two successive reversible steps at −0.02 and 0.25 V (Table 2). Likewise, the reduction occurs in two-step pattern similar to all other compounds: an irreversible wave at −1.69 V due to copper(I) and a irreversible wave at −1.92 V attributable

Table 2
Electrochemical data of **1a–1c**, **3**, **4a–4b**, and **9a–9c**[a]

Compound	Anodic region	Cathodic region
	$E_{1/2}$ (ΔE) (V (mV))	E_{pa} (V)
1a	0.23 (80)	−1.61
1b	0.18 (75)	−1.54
1c	−0.01 (125)	−1.47
3		−1.72 (120)[b]
4a	0.00 (95), 0.26 (100)	−1.48, −1.81
4b	0.02 (80)	−1.53, −1.86
9a	−0.02 (75), 0.25 (105)	−1.69, −1.92
9b	0.05 (90)	−1.73, −1.92
9c	−0.03 (100)	−1.70, −1.92

[a] Recorded on a platinum electrode in dichloromethane solutions (0.5 mM analyte, 0.1 M [Bu$_4$N][PF$_6$]) at 100 mV/s. The potentials are given relative to the ferrocene/ferrocenium reference [20]. Definitions: half-wave potential $E_{1/2} = 1/2(E_{pa} + E_{pc})$, peak separation $\Delta E = E_{pa} - E_{pc}$; E_{pa} and E_{pc} denote anodic and cathodic peaks, respectively.

[b] Reversible reduction; given as: $E_{1/2}$ (ΔE) (V (mV)).

to the Ti(IV)/Ti(III) redox couple (vide supra) [21]. The reduction of **9b** and **9c** occurs in a similar pattern and at similar potentials as described for **9a**. By contrast, however, the 'spaced' compounds undergo only single oxidation within the experimentally accessible region. Again, this difference of the oxidation potentials is in accordance with the properties of the carboxylate part (vide supra).

3. Conclusion

Silver(I) and copper(I) ferrocenecarboxylates readily form heterotrimetallic early-late complexes of structural type $\{[Ti](\mu\text{-}\sigma,\pi\text{-}C\equiv CSiMe_3)_2\}MO_2C\text{-}E\text{-}Fc$ when combined with $[Ti](C\equiv CSiMe_3)_2$ titanocene π-tweezer molecules (E = none, *trans*-CH=CH, CH$_2$CH$_2$; M = Ag, Cu; $[Ti] = (\eta^5\text{-}C_5H_4SiMe_3)_2Ti)$. The use of 1′-(diphenylphosphanyl)-1-ferrocenecarboxylic acid (Hdpf), which posses an additional functionality, allows for an extension of this molecular approach toward heterotetrametallic complexes of type $\{[Ti](\mu\text{-}\sigma,\pi\text{-}C\equiv CSiMe_3)_2\}CuO_2CfcPPh_2M(CO)_5$ (M = Cr, Mo, W).

4. Experimental

4.1. General comments

All reactions were carried out under an atmosphere of purified nitrogen (4.6) using standard Schlenk techniques. Tetrahydrofuran and *n*-hexane were purified by distillation from sodium/benzophenone ketyl; dichloromethane was purified by distillation from calcium hydride. Ethanol was purified by distillation from sodium/diethyl phthalate. Triethylamine was purified by distillation from KOH. Acetonitrile was purified by distillation from P$_2$O$_5$. Celite (purified and annealed, Erg. B.6, Riedel de Haen) was used for filtrations.

Infrared spectra were recorded with a Perkin–Elmer FT-IR spectrometer Spectrum 1000. ^{1}H NMR spectra were recorded with a Bruker Avance 250 spectrometer operating at 250.130 MHz in the Fourier transform mode; ^{13}C{^{1}H} NMR spectra were recorded at 62.860 MHz. Chemical shifts are reported in δ units (parts per million) downfield from tetramethylsilane with the solvent as reference signal (CDCl$_3$: ^{1}H NMR δ = 7.26; ^{13}C{^{1}H} NMR δ = 77.16). ^{31}P{^{1}H} NMR spectra were recorded at 101.255 MHz in CDCl$_3$ with P(OMe)$_3$ as an external standard (δ = 139.0 relative to 85% aqueous H$_3$PO$_4$ (δ = 0.00)). ^{29}Si{^{1}H} NMR spectra were recorded at 49.662 MHz in CDCl$_3$ with tetramethylsilane as an external standard (δ = 0.0). All NMR experiments were carried out at 298 K.

Cyclic voltammograms were recorded in a dried cell purged with purified argon. A platinum wire served as a working electrode and as a counter electrode. A saturated calomel electrode in a separated compartment served as reference electrode. All electrode potentials given in the text are given relative to the redox potential of the ferrocene/ferrocenium couple [20]. The analyzed solutions were

prepared by dissolving the samples in dry dichloromethane containing 0.1 M [Bu$_4$N][PF$_6$] (Fluka, dried under oil-pump vacuum) as the supporting electrolyte to give 0.5 mM analyte solutions. Cyclic voltammograms were recorded using a PGZ 100 instrument (Radiometer).

Melting points were determined using analytically pure samples, sealed off in nitrogen purged capillaries on a Gallenkamp MFB 595 010 M melting point apparatus. Microanalyses were performed by the Institute of Organic Chemistry, Chemnitz, University of Technology (C,H,N-Analysator of the company Foss Heraeus Vario) and partly by the Institute of Inorganic Chemistry, University of Halle (CHNS 932, Leco company).

FcCH=CHCO$_2$H (**1b**) [22], FcCH$_2$CH$_2$CO$_2$H (**1c**) [23], $[Ti](C\equiv CSiMe_3)_2$ (**3**) [24], $\{[Ti](\mu\text{-}\sigma,\pi\text{-}C\equiv CSiMe_3)_2\}$-CuMe (**8**) [25], $[\{(\eta^2\text{-}Me_3SiC\equiv CSiMe_3)CuBr\}_2]$ (**10**) [18], Hdpf [6], and M(CO)$_5$(Hdpf) (**14a–14c**) [11] were prepared according to published procedures. All other chemicals were purchased from commercial suppliers and were used without further purification.

4.2. Synthesis

4.2.1. Synthesis of [FcCO$_2$Ag] (2a)

Silver(I) nitrate (369 mg, 2.17 mmol) was dissolved in 0.25 mL of acetonitrile. 10 mL of ethanol was added. To this reaction solution ferrocenecarboxylic acid (**1a**) (500 mg, 2.17 mmol) and triethylamine (220 mg, 0.3 mL, 2.17 mmol) dissolved in 10 mL of ethanol were slowly dropped. A yellow precipitate was immediately formed. After stirring for 1 h at 25 °C the yellow solid was filtered off washed twice with 10 mL portions of ethanol and dried in *oil-pump vacuum*. The silver(I) carboxylate **2a** was obtained as a yellow solid. Yield: 682 mg (2.03 mmol, 93% based on **1a**).

Mp. 100 °C (dec.). IR (KBr, cm^{-1}): 3100 (w), 2962 (w), 2925 (w), 2853 (w), 1540 (vs) v_{as}(CO), 1467 (s), 1388 (s), 1359 (m), 1344 (m), 1261 (m), 1183 (w), 1106 (m), 1059 (w) 1022 (m), 820 (m), 801 (m), 553 (w), 511 (w), 485 (w), 473 (w), 435 (w). Due to insolubility in common NMR-solvents, no NMR spectra of **3** could be recorded. Anal. Calc. for C$_{11}$H$_9$AgFeO$_2$ (336.90): C, 39.20; H, 2.69. Found: C, 39.10; H, 3.01%.

4.2.2. Synthesis of [FcCH=CHCO$_2$Ag] (2b)

FcCH=CHCO$_2$H (**1b**) (215 mg, 0.78 mmol) and triethylamine (0.3 mL, 2.17 mmol) dissolved in 10 mL of ethanol were slowly added to a stirred solution of [AgNO$_3$] (142 mg, 0.84 mmol) in acetonitrile (0.5 mL) at room temperature. A red-brown precipitate was immediately formed, and after 45 min of stirring, it was filtered off, washed with 10 mL of ethanol and dried in *oil-pump vacuum* to afford **2b** as a red-brown solid, insoluble in common organic solvents. Yield: 279 mg (0.77 mmol, 99% based on **1b**).

Mp. 120 °C (dec.). IR (KBr, cm^{-1}): 1639 (s) v(C=C), 1562 (vs) v_{as}(CO), 1400 (s), 1382 (s), 1286 (w), 1259 (w),

1106 (w), 1046 (w), 1030 (w), 999 (w), 815 (w), 670 (w), 487 (w), 477 (w). Due to insolubility in common NMR-solvents no NMR spectra of **2b** could be recorded. Anal. Calc. for $C_{13}H_{11}AgFeO_2$ (362.92): C, 43.02; H, 3.06. Found: C, 42.72; H, 3.46%.

4.2.3. Synthesis of {[Ti](μ-σ,π-C≡CSiMe₃)₂}AgO₂CFc (4a)

[Ti](C≡CSiMe₃)₂ (**3**) (238 mg, 0.46 mmol) was dissolved in 30 mL of tetrahydrofuran. To this solution [FcCO₂Ag] (**2a**) (155 mg, 0.46 mmol) was added in a single portion. The reaction solution was allowed to stirr for 2 h at 25 °C. Afterward it was filtered through a pad of Celite. Removal of all volatiles in *oil pump vacuum* gave an orange solid. Yield: 365 mg (0.427 mmol; 92.8% based on **2a**).

Mp. 110 °C. IR (KBr, cm⁻¹): 3058 (w), 2955 (w), 2896 (w), 1948 (w) v(C≡C), 1570 (s) v_{as}(CO), 1466 (s), 1408 (w), 1381 (s), 1339 (m), 1247 (s), 1176 (m), 1104 (w), 1048 (m), 1020 (w), 1001 (w), 902 (m), 841 (vs), 756 (s), 672 (s), 634 (w), 606(w), 505 (w). ^{1}H NMR (CDCl₃): δ 0.24 (s, 18H, C≡CSi*Me₃*), 0.25 (s, 18H, C₅H₄Si*Me₃*), 4.18 (pt, J_{HH} = 1.8 Hz, 2H, C₅*H₄*), 4.2 (s, 5H, C₅*H₅*), 4.71 (pt, J_{HH} = 1.8 Hz, 2H, C₅*H₄*), 6.22 (pt, J_{HH} = 2.3 Hz, 4H, C₅*H₄*SiMe₃), 6.27 (pt, J_{HH} = 2.3 Hz, 4H, C₅*H₄*SiMe₃). ^{13}C{^{1}H} NMR (CDCl₃): δ 0.2 (C≡CSi*Me₃*), 0.5 (C₅H₄Si*Me₃*), 69.1 (C₅*H₅*), 69.2(*C*H/C₅H₄), 70.5 (*C*H/C₅H₄), 79.7 (^{i}*C*/C₅H₄), 116.3 (C₅H₄SiMe₃), 118.5(C₅H₄-SiMe₃), 124.4 (^{i}*C*/C₅H₄SiMe₃), 138.3 (d, J_{AgC} = 6.2 Hz, Ti*C*≡CSiMe₃), 155.4 (d, J_{AgC} = 15.4 Hz, TiC≡*C*SiMe₃), 175.8 (*C*O₂). ^{29}Si{^{1}H} NMR (CDCl₃): δ −17.9 (d, J_{AgSi} = 2.8 Hz, C≡C*Si*Me₃), −5.7 (C₅H₄*Si*Me₃). Anal. Calc. for $C_{37}H_{53}AgFeO_2Si_4Ti$ (853.72): C, 52.05; H, 6.26. Found: C, 51.33, H, 6.20%.

4.2.4. Synthesis of {[Ti](μ-σ,π-C≡CSiMe₃)₂}-AgO₂CCH=CHFc (4b)

[Ti](C≡CSiMe₃)₂ (**3**) (326 mg, 0.63 mmol) was dissolved in 15 mL of tetrahydrofuran and [FcCH=CHCO₂Ag] (**2b**) (230 mg, 0.63 mmol) was added in one portion. The reaction solution was stirred for 2 h at 25 °C, while the color changed from orange to red. Afterward it was filtered through a pad of Celite. All volatiles were removed in *oil pump vacuum* to gave **4b** as a red-brown solid. Yield: 519 mg (0.59 mmol, 94% based on **2b**).

Mp. 99 °C (dec.). IR (KBr, cm⁻¹): 2953 (m), 2896 (w), 1942 (w) v(C≡C), 1637 (m) v(C=C), 1552 (s) v_{as}(CO), 1400 (s), 1375 (s), 1246 (s), 1176 (w), 1045 (w), 902 (w), 840 (vs), 756 (m), 672 (s), 495 (w). ^{1}H NMR (CDCl₃): δ 0.23 (s, 18H, Si*Me₃*), 0.24 (s, 18H, Si*Me₃*), 4.09 (s, 5H, C₅*H₅*), 4.22 (pt, J_{HH} = 1.8 Hz, 2H, C₅*H₄*), 4.42 (pt, J_{HH} = 1.8 Hz, 2H, C₅*H₄*), 6.23 (m, 8H, C₅*H₄*SiMe₃), 6.26 (d, $^2J_{HH}$ = 15.5 Hz, 1H, =C*H*), 7.27 (d, $^2J_{HH}$ = 15.5 Hz, 1H, =C*H*). ^{13}C{^{1}H} NMR (CDCl₃): δ 0.2 (*C*H₃), 0.3 (*C*H₃), 68.0 (*C*H/C₅H₄), 69.4 (C₅*H₅*), 69.5 (*C*H/C₅H₄), 81.4 (^{i}*C*/C₅H₄), 116.7 (*C*H/C₅H₄SiMe₃), 118.6 (*C*H/C₅H₄SiMe₃), 122.8 (=*C*H), 124.3 (^{i}*C*/C₅H₄SiMe₃), 137.4 (d, J_{AgC} = 7 Hz, Ti*C*≡CSiMe₃), 138.4 (=*C*H), 156.0 (d,

J_{AgC} = 15 Hz, Ti*C*≡CSiMe₃), 173.2 (*C*OOH). ^{29}Si{^{1}H} NMR (CDCl₃): δ −17.9 (d, J_{AgSi} = 2 Hz, Me₃SiC≡C), −5.7 (Me₃*Si*C₅H₄). Anal. Calc. for $C_{39}H_{55}AgFeO_2Si_4Ti$ (879.75): C, 53.24; H, 6.30. Found: C, 53.19; H, 6.00%.

4.2.5. Synthesis of [Ag(dpf)]₄ (5)

Silver(I) nitrate (160 mg, 0.94 mmol) was dissolved in 0.15 mL of acetonitrile and afterward 10 mL of ethanol was added. To this solution Hdpf (390 mg, 0.94 mmol) and triethylamine (119 mg, 0.15 mL, 1.08 mmol) in 10 mL of ethanol were slowly added, whereby a yellow precipitate immediately formed. After stirring for 1 h at 25 °C the solvent was reduced to a volume of 10 mL and the yellow solid was filtered off washed twice with 5 mL portions of ethanol and dried in *oil-pump vacuum* to gave yellow **5**. Yield: 318 mg (0.61 mmol, 65% based on Hdpf).

Mp. 181 °C. IR (KBr, cm⁻¹): 1560 (vs) v_{as}(CO), 1542 (vs), 1461 (m), 1436 (m), 1386 (s), 1350 (m), 1167 (m), 1093 (m), 1027 (m), 743(m), 694 (m), 503 (m), 465 (m), 441 (m), 418 (m). ^{1}H NMR (CDCl₃): δ 4.05 (bs, 2H, C₅*H₄*), 4.30 (bs, 2H, C₅*H₄*), 4.59 (bs, 2H, C₅*H₄*), 4.85 (bs, 2H, C₅*H₄*), 7.32–7.68 (m, 10H, Ph). ^{13}C{^{1}H} NMR (CDCl₃): δ 70.6 (*C*H/C₅H₄), 72.6 (*C*H/C₅H₄), 72.7 (*C*H/C₅H₄), 73.4 (*C*H/C₅H₄), 75.0 (d, $^1J_{PC}$ = 15 Hz, ^{i}*C*/C₅H₄), 78.2 (^{i}*C*/C₅H₄), 128.9 (d, J_{PC} = 11.0 Hz, *C*H/Ph), 130.7 (*C*H/Ph), 133.8 (d, J_{PC} = 16.8 Hz, *C*H/Ph), 171.8 (*C*O₂), the signal of ^{i}*C*/Ph could not be detected. ^{31}P{^{1}H} NMR (CDCl₃): δ 5.1 (d, $^1J_{109Ag31P}$ = 790.0 Hz), 5.1 (d, $^1J_{107Ag31P}$ = 668.7 Hz). Anal. Calc. for $C_{23}H_{18}AgFeO_2P$ (521.06): C, 53.01; H, 3.48. Found: C, 51.97; H, 3.69%.

4.2.6. Synthesis of [Ag(dpf)(Hdpf)] (7)

Using the same procedure and the same amounts of the starting materials like for the preparation of **5**, but running the reaction in a mixture of Et₂O/EtOH (6:1) gave **7** as a yellow solid. Yield: 353 mg (0.38 mmol, 81% based on Hdpf).

Mp. 176 °C. IR (KBr, cm⁻¹): 3351 (m) v(OH), 3053 (w), 2963 (w), 2859 (w), 1637 (s) v_{as}(CO), 1561 (m), 1546 (m), 1479 (s), 1436 (s), 1383 (s), 1337 (m), 1310 (m), 1268 (w), 1199 (w), 1170 (s), 1096 (s), 1070 (w), 1052 (w), 1029 (s), 999 (w), 916 (w), 877 (w), 831 (m), 804 (m), 742 (s), 694 (s), 632 (w), 538 (w), 498 (s). ^{1}H NMR (CDCl₃): δ 4.04 (pt, J_{HH} = 1.9 Hz, 4H, C₅*H₄*), 4.53 (bs, 4H, C₅*H₄*), 4.62 (pt, J_{HH} = 1.7 Hz, 4H, C₅*H₄*), 4.84 (pt, J_{HH} = 1.9 Hz, 4H, C₅*H₄*), 7.20–7.53 (m, 24H, Ph). ^{13}C{^{1}H} NMR (CDCl₃): δ 71.2 (C₅*H₄*), 73.0 (C₅*H₄*), 75.4 (C₅*H₄*), 76.4 (C₅*H₄*), 128.7 (m, Ph), 130.2 (Ph), 134.0 (m, Ph), 178.2 (*C*O₂). ^{31}P{^{1}H} NMR (CDCl₃): δ −1.8 (d, $^1J_{109Ag31P}$ = 526.1 Hz), −1.8 (d, $^1J_{107Ag31P}$ = 455.9 Hz). Anal. Calc. for $C_{46}H_{37}AgFe_2O_4P_2$ (935.25): C, 59.07; H, 3.99. Found: C, 58.73; H, 4.59%.

4.2.7. Synthesis of {[Ti](μ-σ,π-C≡CSiMe₃)₂}-CuO₂CFc (9a)

Method 1: [(η²-Me₃SiC≡CSiMe₃)(CuO₂CFc)₂]₂ (**11**) (37 mg, 0.02 mmol) was dissolved in 20 mL of tetrahydro-

furan. [Ti](C≡CSiMe$_3$)$_2$ (**3**) (41 mg, 0.08 mmol) was added in a single portion at 25 °C. The dark red solution was stirred for 1 h and was then evaporated to dryness in *oil-pump vacuum*. The residue was washed twice with 5 mL portions of *n*-hexane and dried in *oil-pump vacuum*. Complex **9a** was obtained as an orange solid. Yield: 57 mg (0.07 mmol, 87% based on **11**).

Method 2: {[Ti](μ-σ,π-C≡CSiMe$_3$)$_2$}CuMe (**8**) (85 mg, 0.14 mmol) was dissolved in 20 mL of tetrahydrofuran and cooled to −30 °C. To this solution FcCO$_2$H (**1a**) (33 mg, 0.14 mmol) in 5 mL of tetrahydrofuran was added dropwise over a period of 5 min. The resulting solution was stirred for 30 min at −30 °C and then for 1 h at 25 °C. The solvent was evaporated in *oil-pump vacuum* and the residue was extracted with *n*-hexane (15 mL) and filtered through a pad of Celite. After evaporation of the solvent in *oil-pump vacuum*, compound **9a** was obtained as an orange solid. Yield: 108 mg (0.13 mmol, 93% based on **1a**).

Mp. 149 °C (dec.). IR (KBr, cm^{-1}): 2953 (m), 2895 (w), 1915 (w) ν(C≡C), 1584 (s), ν_{as}(CO), 1458 (s), 1380 (s), 1331 (s), 1246 (s), 1176 (w), 1051 (w), 902 (w), 841 (vs), 757 (m), 681 (m). ^{1}H NMR (CDCl$_3$): δ 0.24 (s, 18H, C≡CSi*Me$_3$*), 0.25 (s, 18 H,C$_5$H$_4$Si*Me$_3$*), 4.19–4.21 (m, 7H, C$_5$*H$_4$*, C$_5$*H$_5$*), 4.66 (pt, J_{HH} = 1.7 Hz, 2H, C$_5$*H$_4$*), 6.01 (pt, J_{HH} = 2.3 Hz, 4H, C$_5$*H$_4$*SiMe$_3$), 6.1 (pt, J_{HH} = 2.3 Hz, 4H, C$_5$*H$_4$*SiMe$_3$). ^{13}C{^{1}H} NMR (CDCl$_3$): δ 0.3 (*C*H$_3$), 0.5 (*C*H$_3$), 69.1 (*C$_5$*H$_5$), 69.2 (*C$_5$*H$_4$), 69.3 (*C$_5$*H$_4$), 69.3 (*C$_5$*H$_4$), 113.7 (*C*H/C$_5$H$_4$SiMe$_3$), 116.5 (*C*H/C$_5$H$_4$SiMe$_3$), 121.9 (*^{i}C*/C$_5$H$_4$SiMe$_3$), 133.5 (Ti*C*≡CSiMe$_3$), 170.5 (Ti*C*≡CSiMe$_3$). Please, notice that the HO$_2$*C*H signal could not be detected. ^{29}Si{^{1}H} NMR (CDCl$_3$): δ −15.4 (*C*≡CSiMe$_3$), −6.0 (C$_5$H$_4$*Si*Me$_3$). Anal. Calc. for C$_{37}$H$_{53}$-CuFeO$_2$Si$_4$Ti (809.39): C, 54.90; H, 6.60. Found: C, 54.27, H, 6.20%.

4.2.8. Synthesis of {[Ti](μ-σ,π-C≡CSiMe$_3$)$_2$}-CuO$_2$CCH=CHFc (9b)

FcCH=CHCO$_2$H (**1b**) (52 mg, 0.20 mmol) dissolved in 20 mL of tetrahydrofuran was added dropwise to a stirred solution of {[Ti](μ-σ,π-C≡CSiMe$_3$)$_2$}CuMe (**8**) (120 mg, 0.20 mmol) in 20 mL of the same solvent at −30 °C during 5 min. The reaction solution was stirred for 30 min at −30 °C and then 1 h at 25 °C. Evaporation of the solvent in *oil-pump vacuum* afforded **9b** as a red solid. Yield: 167 mg (0.20 mmol, 100% based on **1b**).

Mp. 108–110 °C (dec.). IR (KBr, cm^{-1}): 2953 (m), 2896 (m), 1915 (w) ν(C≡C), 1637 (s) ν(C=C), 1571 (w) ν_{as}(CO), 1463 (w), 1403 (s), 1374 (m), 1246 (s), 1176 (w), 1047 (w), 903 (w), 842 (vs), 757 (m), 679 (m), 496 (w). ^{1}H NMR (CDCl$_3$): δ 0.24 (s, 18H, C*H$_3$*), 0.26 (s, 18H, C*H$_3$*), 4.11 (s, 5H, C$_5$H$_5$), 4.28 (bs, 2H, C$_5$H$_4$), 4.46 (bs, 2H, C$_5$H$_4$), 5.98 (pt, J_{HH} = 2.3 Hz, 4H, C$_5$H$_4$SiMe$_3$), 6.11 (pt, J_{HH} = 2.3 Hz, 4H, C$_5$H$_4$SiMe$_3$), 6.24 (bd, $^3J_{HH}$ = 17 Hz, 1H, =C*H*), 7.31 (bd, ^3J = 17 Hz, 1H, =C*H*). ^{13}C{^{1}H} NMR (CDCl$_3$): δ 0.4 (*C*H$_3$), 0.5 (*C*H$_3$), 68.4 (*C*H/C$_5$H$_4$), 69.7 (*C$_5$*H$_5$), 70.1 (*C*H/C$_5$H$_4$), 113.5 (*C*H/C$_5$H$_4$SiMe$_3$), 116.5 (*C*H/C$_5$H$_4$SiMe$_3$), 121.8 (*^{i}C*/C$_5$H$_4$SiMe$_3$), 132.6 (Ti*C*≡CSiMe$_3$), 171.3

(Ti*C*≡CSiMe$_3$), the signals for ^{i}*C*/C$_5$H$_4$, 2× =CH, and HO$_2$C could not be detected. ^{29}Si{^{1}H} NMR (CDCl$_3$): δ −15.5 (Me$_3$SiC≡C), −6.0 (Me$_3$SiC$_5$H$_4$). Anal. Calc. for C$_{39}$H$_{55}$CuFeO$_2$Si$_4$Ti (835.43): C, 56.07; H, 6.64. Found: C, 56.24, H, 6.54%.

4.2.9. Synthesis of {[Ti](μ-σ,π-C≡CSiMe$_3$)$_2$}-CuO$_2$CCH$_2$CH$_2$Fc (9c)

FcCH$_2$CH$_2$CO$_2$H (**1c**) (52 mg, 0.20 mmol) was reacted with {[Ti](μ-σ,π-C≡CSiMe$_3$)$_2$}CuMe (**8**) (120 mg, 0.20 mmol) under similar conditions as described for the synthesis of **9b**. After evaporation of the solvent, the residue was extracted into 10 mL of *n*-hexane and filtered under nitrogen through a pad of Celite. Removal of the solvent in *oil-pump vacuum* gave **9c** as a red-brown waxy solid. Yield: 143 mg (0.17 mmol, 85% based on **1c**).

IR (NaCl, cm^{-1}): 3094 (w), 2962 (s), 2927 (m), 2905 (m), 2856 (w), 1916 (w) ν(C≡C), 1716 (w) ν_{as}(CO), 1583–1557 (composite m) ν(C=C), 1446 (w), 1410 (m), 1374 (w), 1260 (s), 1177 (w), 1104–1022 (composite s), 903 (w), 800 (composite s), 759 (m), 698 (m), 635 (w). ^{1}H NMR (CDCl$_3$): δ 0.25 (s, 36H, C*H$_3$*), 2.63 (m, 4H, C*H$_2$*), 4.03 (bs, 2H, C$_5$H$_4$), 4.09 (m, 7H, C$_5$*H$_4$* and C$_5$*H$_5$*), 6.00 (bs, 4H, C$_5$H$_4$SiMe$_3$), 6.11 (bs, 4H, C$_5$H$_4$SiMe$_3$). ^{13}C{^{1}H} NMR (CDCl$_3$): δ 0.3 (*C*H$_3$), 1.2 (*C*H$_3$), 67.2 (*C*H/C$_5$H$_4$), 68.1 (*C*H/C$_5$H$_4$), 68.6 (*C$_5$*H$_5$), 89.2 (*^{i}C*/C$_5$H$_4$), 113.6 (*C*H/C$_5$H$_4$SiMe$_3$), 116.5 (*C*H/C$_5$H$_4$SiMe$_3$), 121.9 (*^{i}C*/C$_5$H$_4$SiMe$_3$), 132.8 (Ti*C*≡C-SiMe$_3$), 170.7 (Ti*C*≡CSiMe$_3$), the signals of CH$_2$ and COOH could not be detected. ^{29}Si{^{1}H} NMR (CDCl$_3$): δ −15.6 (Me$_3$*Si*C≡C), −6.0 (Me$_3$*Si*C$_5$H$_4$). Anal. Calc. for C$_{39}$H$_{57}$CuFeO$_2$Si$_4$Ti (837.45): C, 55.93; H, 6.86. Found: C, 55.05; H, 7.54%.

4.2.10. Synthesis of [(η^2-Me$_3$SiC≡CSiMe$_3$)-(CuO$_2$CFc)$_2$]$_2$ (11)

[(η^2-Me$_3$SiC≡CSiMe$_3$)CuBr]$_2$ (**10**) (280 mg, 0.446 mmol) was dissolved in 70 mL of tetrahydrofuran and afterward this solution was cooled to 0 °C. [FcCO$_2$Ag] (**2a**) (300.0 mg, 0.892 mmol) was added in a single portion. The reaction mixture was stirred for 3 h at 0 °C and was then filtered through a pad of Celite. The filtrate was evaporated to dryness in *oil-pump vacuum* and the remaining solid was washed three times with 5 mL portions of *n*-hexane and dried in *oil-pump vacuum*. Complex **11** was obtained as an orange solid. Yield: 517 mg (0.342 mmol; 76.7% based on **2a**).

Mp. 128 °C (dec.). IR (KBr, cm^{-1}): 2960 (w), 2899 (w), 1958 (w) ν(C≡C), 1586 (vs) ν_{as}(CO), 1481 (s), 1388 (s), 1361 (m), 1248 (m), 1194 (w), 1106 (m), 1074 (w), 1022 (m), 1001 (w), 847 (vs), 786 (m), 759 (m), 701 (w), 527 (w). ^{1}H NMR (CDCl$_3$): δ 0.43 (s, 36H, C*H$_3$*), 4.10 (s, 20H, C$_5$H$_5$), 4.19 (pt, J_{HH} = 1.7 Hz, 8H, C$_5$H$_4$), 4.65 (pt, J_{HH} = 1.7 Hz, 8H, C$_5$H$_4$). ^{13}C{^{1}H} NMR: δ 0.5 (*C*H$_3$), 69.4 (*C$_5$*H$_5$), 70.0 (*C*H/C$_5$H$_4$), 70.6 (*C*H/C$_5$H$_4$). The signals for ^{i}*C*/C$_5$H$_4$, ≡C, and HO$_2$C could not be detected. ^{29}Si{^{1}H} NMR (CDCl$_3$): δ −5.6. ESI-MS [*m/z* (relative

intensities)]: [M$^+$−Me$_3$SiC≡CSiMe$_3$−Cu] 1277 (100). Anal. Calc. for C$_{60}$H$_{72}$Cu$_4$Fe$_4$O$_8$Si$_4$ (1511.08): C, 47.69; H, 4.80. Found: C, 47.78; H, 5.10%.

4.2.11. Synthesis of {[Ti](µ-σ,π-C≡CSiMe$_3$)$_2$}-CuO$_2$CfcPPh$_2$ (12)

Hdpf (75 mg, 0.18 mmol) dissolved in 15 mL of tetrahydrofuran was added dropwise to a stirred solution of {[Ti](µ-σ,π-C≡CSiMe$_3$)$_2$}CuMe (8) (107 mg, 0.18 mmol) in 15 mL of the same solvent at −60 °C. The reaction mixture was stirred for 30 min at −60 °C and then for 2 h at 25 °C. Evaporation of all volatiles in *oil-pump vacuum* afforded 12 as an orange solid. Yield: 179 mg (0.18 mmol, 100% based on Hdpf).

Mp. 89–91 °C (dec.). IR (KBr, cm^{-1}): 3066 (w), 2952 (m), 2893 (m), 1915 (w) *v*(C≡C), 1586 (m) *v*$_{as}$(CO), 1463 (m), 1433 (w), 1388 (m), 1333 (m), 1245 (s), 1177 (w), 1094 (w), 1048 (m), 1023 (m), 903 (w), 839 (vs), 755 (m), 696 (m), 677 (m), 499 (w). ^{1}H NMR (CDCl$_3$): δ 0.20 (s, 18H, C*H*$_3$), 0.24 (s, 18H, C*H*$_3$), 4.09 (bs, 2H, C$_5$*H*$_4$), 4.14 (bs, 2H, C$_5$*H*$_4$), 4.48 (bs, 2H, C$_5$*H*$_4$), 4.56 (bs, 2H, C$_5$*H*$_4$), 5.99 (pt, *J*$_{HH}$ = 2.3 Hz, 4H, C$_5$*H*$_4$SiMe$_3$), 6.09 (pt, *J*$_{HH}$ = 2.3 Hz, 4H, C$_5$*H*$_4$SiMe$_3$), 7.20–7.40 (m, 10H, Ph). ^{13}C{^{1}H} NMR (CDCl$_3$): δ 0.3 (*C*H$_3$), 0.4 (*C*H$_3$), 70.9 (*C*H/C$_5$H$_4$), 71.1 (br s, *C*H/C$_5$H$_4$), 72.8 (*C*H/C$_5$H$_4$), 73.7

(br s, *C*H/C$_5$H$_4$), 81.9 (br s, ^{i}*C*/C$_5$H$_4$), 113.7 (*C*H/C$_5$H$_4$SiMe$_3$), 116.5 (*C*H/C$_5$H$_4$SiMe$_3$), 121.9 (^{i}*C*/C$_5$H$_4$SiMe$_3$), 127.2, 128.3, 128.7, 131.5 (Ph), 133.3 (Ti*C*≡CSiMe$_3$), 133.5, 133.7, 134.7, 139.2 (Ph), 170.3 (Ti*C*≡CSiMe$_3$), 175.5 (*C*OOH). The signal for the ^{i}C/C$_5$H$_4$ carbon atom could not be detected. ^{31}P{^{1}H} NMR (CDCl$_3$): δ −17.9 (s). ^{29}Si{^{1}H} NMR (CDCl$_3$): δ −15.5 (Me$_3$SiC≡C), −6.0 (Me$_3$SiC$_5$H$_4$). Anal. Calc. for C$_{49}$H$_{62}$CuFeO$_3$PSi$_4$Ti (1009.56): C, 58.29; H, 6.19. Found: C, 58.12; H, 6.69%.

4.2.12. Synthesis of {[Ti](µ-σ,π-C≡CSiMe$_3$)$_2$}-CuO$_2$CfcPPh$_2$[Mo(CO)$_5$] (15b)

The same procedure as for 12, (Hdpf)Mo(CO)$_5$ (14b) (40 mg, 0.06 mmol) in 15 mL of tetrahydrofuran is used and reacted with {[Ti](µ-σ,π-C≡CSiMe$_3$)$_2$}CuMe (8). Compound 15b was obtained as a brown solid. Yield: 59 mg (96% based on 14b).

Mp. 123 °C (dec.). IR (KBr, cm^{-1}): 2070 (s) *v*(CO), 1986 (s) *v*(CO), 1945 (vs), 1922 (sh) *v*(CO), 1604 (m), 1591 (m) *v*$_{as}$(CO), 1335 (m), 1246 (m), 1176 (w), 1163 (w), 1095 (w), 1049 (w), 1030 (w), 903 (w), 839 (composite s), 757 (w), 737 (w), 696 (w), 677 (w), 608 (w), 587 (m). ^{1}H NMR (CDCl$_3$): δ 0.18 (s, 18H, C*H*$_3$), 0.24 (s, 18H, C*H*$_3$), 4.00 (bs, 2H, C$_5$*H*$_4$), 4.30 (bs, 2H, C$_5$*H*$_4$), 4.44 (bs, 2H,

Table 3
Crystal and intensity collection data for compounds 5, 7, 9a, and 11

Compound	5	7	9a	11
Formula weight	648.45	820.80	2128.44	755.55
Chemical formula	C$_{24.5}$H$_{21}$AgCl$_3$FeO$_2$P	C$_{41}$H$_{35}$AgClFeO$_2$P$_2$	C$_{80}$H$_{118}$Cl$_{12}$Cu$_2$Fe$_2$O$_4$Si$_8$Ti$_2$	C$_{30}$H$_{36}$Cu$_2$Fe$_2$O$_4$Si$_2$
Crystal system	Tetragonal	Tetragonal	Triclinic	Triclinic
Space group	P4$_2$/n (no. 86)	I4$_1$ (no. 80)	P$\bar{1}$ (no. 2)	P$\bar{1}$ (no. 2)
a (Å)	13.7539(4)	17.8803(4)	16.7085(6)	11.346(3)
b (Å)	13.7539(4)	17.8803(4)	17.0597(8)	12.220(4)
c (Å)	26.8981(17)	13.2474(7)	20.1037(9)	13.539(3)
α (°)	90	90	115.027(4)	69.293(7)
β (°)	90	90	95.616(4)	80.638(10)
γ (°)	90	90	90.025(3)	82.822(9)
V (Å^3)	5088.3(4)	4235.3(3)	5161.9(4)	1727.8(8)
ρ$_{calc}$ (g cm^{-3})	1.693	1.287	1.369	1.452
F(000)	2584	1168	2200	772
Crystal size dimensions (mm)	0.4 × 0.3 × 0.3	0.3 × 0.2 × 0.2	0.4 × 0.2 × 0.2	0.3 × 0.3 × 0.2
Z	8	4	2	2
T-range transmission	0.672–1.000	0.844–1.000	–^{d}	0.813–1.000
µ (mm^{-1})	1.738	0.973	1.271	2.136
T (K)	183(2)	183(2)	100(2)	298(2)
θ Range (°)	1.51–26.47	1.61–26.42	2.84–24.69	1.62–27.90
Total reflections	25 680	23 236	38 059	20 194
Unique reflections	5396	4355	17 053	8161
R$_{int}$^{a}	5.84	2.00	4.35	2.19
Data/restraints/parameters	5257/34/322	4347/1/265	17053/0/981	8161/0/368
S^b	1.071	1.044	0.883	1.013
R, wR [I ⩾ ^{3}σ(I)]^c	4.49, 10.0	1.91, 5.07	6.08, 15.6	2.58, 6.57
R, wR (all data)^c	6.92, 11.3	2.01, 5.13	11.5, 16.9	3.70, 7.04
Δρ (e Å^{-3})	0.744, −0.764	0.209, −0.442	1.204, −0.896	0.475, −0.374

^{a} $R_{int} = \sum||F_o^2| - |F_o^2(\text{mean})||/\sum F_o^2$, where $F_o^2(\text{mean})$ is the average intensity of symmetry-equivalent diffractions.

^{b} $S = [\sum w(F_o^2 - F_c^2)^2]/(n - p)]^{1/2}$, where n = number of reflections, p = number of parameters.

^{c} $R = [\sum(||F_o| - |F_c||)/\sum|F_o|]$; $wR = [\sum(w(F_o^2 - F_c^2)^2)/\sum(wF_o^4)]^{1/2}$.

^{d} Not corrected.

C_5H_4), 4.61 (bs, 2H, C_5H_4), 6.00 (m, 4H, C_5H_4SiMe$_3$), 6.10 (m, 4H, C_5H_4SiMe$_3$), 7.35–7.55 (m, 10H, Ph). ^{13}C{^{1}H} NMR (CDCl$_3$): δ 0.3 (CH_3), 0.4 (CH_3), 71.0 (d, $J_{PC} = 2$ Hz, CH/C_5H_4), 71.3 (CH/C_5H_4), 74.0 (d, $J_{PC} = 2$ Hz, CH/C_5H_4), 74.2 (d, $J_{PC} = 8$ Hz, CH/C_5H_4), 113.8 (CH/C_5H_4SiMe$_3$), 116.6 (CH/C_5H_4SiMe$_3$), 122.1 ($^iC/C_5H_4$SiMe$_3$), 128.2 (d, $^1J_{PC} = 9$ Hz, $CH/$Ph), 129.8 (d, $J_{PC} = 2$ Hz, $CH/$Ph), 132.6 (d, $J_{PC} = 12$ Hz, Ph), 133.5 (Ti$C\equiv C$SiMe$_3$), 138.4 (d, $J_{PC} = 38$ Hz, $^iC/$PPh$_2$), 170.1 (Ti$C\equiv C$SiMe$_3$), 206.0 (d, $^2J_{PC} = 9$ Hz, CO). The signals for $^iC/C_5H_4$, HO$_2$C and *axial-C*O could not be detected. ^{31}P{^{1}H} NMR (CDCl$_3$): δ 26.7 (s). ^{29}Si{^{1}H} NMR (CDCl$_3$): δ −15.5 (Me$_3$$SiC\equiv$C), −6.0 (Me$_3$$SiC_5H_4$). Due to the high instability of this compound no satisfactory elemental analysis could be obtained.

4.3. Crystal structure determination

Crystal data for **5**, **7**, **9a**, and **11** are presented in Table 3. All data were collected on a Bruker Smart CCD 1k diffractometer at 298(2) K (**11**) or 183(2) K (**5**, **7**) or on an Oxford Gemini diffractometer at 100(2) K (**9a**) using oil-coated shock-cooled crystals [26] using Mo Kα radiation ($\lambda = 0.71073$ Å). The structures were solved by direct methods using SHELXS-97 [27] and refined by full-matrix least-square procedures on F^2 using SHELXL-97 [28]. All non-hydrogen atoms were refined anisotropically, and a riding model was employed in the refinement of the hydrogen atom positions. In **5** a dichloromethane molecule is disordered and has been refined to split occupancies of 0.54/0.46. In **11** the asymmetric unit contains a *non*-definable solvent molecule. The electron density has been deducted from the electron density map by the SQUEEZE procedure implemented in PLATON-94 (vide supra) [29]. In **7** the asymmetric unit contains half of the molecule. The second part is generated by the crystallographic C$_2$-axis.

Acknowledgements

References

[1] (a) P. Kaszynski, J. Michl, J. Am. Chem. Soc. 110 (1988) 5225;
(b) P. Kaszynski, A.C. Friedli, J. Michl, J. Am. Chem. Soc. 114 (1992) 601.
[2] F. Stoddard, Chem. Ber. 24 (1988) 1203.
[3] F.M. Raymo, J.F. Stoddart, Chem. Rev. 99 (1999) 1643.
[4] H. Lang, R. Packheiser, B. Walfort, Organometallics 25 (2006) 1836.
[5] (a) For example: J. Haijun, C. Karine, J.A. Gladysz, J.-F. Halet, M. Guillemot, L. Toupet, F. Paul, C. Lapinte, J. Am. Chem. Soc. 125 (2003) 9511;
(b) W. Skibar, H. Kopacka, K. Wurst, C. Salzmann, K.-H. Ongania, F.F. de Biani, P. Zanello, B. Bildstein, Organometallics 23 (2004) 1024;
(c) C.L. Sterzot, J.K. Stille, Organometallics 9 (1990) 687;
(d) A. Mayboroda, P. Comba, H. Pritzkow, G. Rheinwald, H. Lang, G. van Koten, Eur. J. Inorg. Chem. (2003) 1703.
[6] (a) J. Podlaha, P. Štěpnička, I. Císařová, J. Ludvík, Organometallics 15 (1996) 543;
(b) P. Štěpnička, Eur. J. Inorg. Chem. (2005) 3787.
[7] N.G. Connelly, W.E. Geiger, Chem. Rev. 96 (1998) 877.
[8] (a) H. Lang, D.S.A. George, G. Rheinwald, Coord. Chem. Rev. 206–207 (2000) 101;
(b) H. Lang, K. Köhler, S. Blau, Coord. Chem. Rev. 143 (1995) 113.
[9] Z. Yuan, N.H. Dryden, J.J. Vittal, R.J. Puddephatt, Chem. Mater. 7 (1995) 1696.
[10] W. Strohmeier, F.-J. Müller, Chem. Ber. 102 (1969) 3608.
[11] L. Lukešová, J. Ludvík, I. Císařová, P. Štěpnička, Collect. Czech. Chem. Commun. 65 (2000) 1897.
[12] J.E.D. Kirkham, T.D.L. Courtney, V. Lee, J.E. Baldwin, Tetrahedron 61 (2005) 7219.
[13] P. Štěpnička, J. Demel, J. Čejka, J. Mol. Catal. A 224 (2004) 161.
[14] W. Frosch, S. Back, H. Müller, K. Köhler, A. Driess, B. Schiemenz, G. Huttner, H. Lang, J. Organomet. Chem. 619 (2001) 99.
[15] W. Frosch, S. Back, G. Rheinwald, K. Köhler, L. Zsolnai, G. Huttner, H. Lang, Organometallics 19 (2000) 5769.
[16] G. Rabe, A.L. Rheingold, C.D. Incarvito, Z. Kristallogr. 215 (2000) 560.
[17] M. Bardet, M.F. Foray, S. Li, K. Lundquist, R. Stombert, J. Chem. Crystallogr. 29 (1999) 1023.
[18] H. Lang, K. Köhler, L. Zsolnai, Chem. Ber. 128 (1995) 519.
[19] (a) T.C.H. Lam, W.-L. Mak, W.-L. Wong, H.L. Kwong, H.H.Y. Sung, S.M.F. Lo, I.D. Williams, W.-H. Leung, Organometallics 23 (6) (2004) 1247;
(b) C.W. Baxter, T.C. Higgs, A.C. Jones, S. Parsons, P.J. Bailey, P.A. Tasker, J. Chem. Soc., Dalton Trans. (2002) 4395;
(c) P. Doppelt, T.H. Baum, J. Organomet. Chem. 517 (1996) 53.
[20] (a) A conversion of given electrode potentials to the standard normal hydrogen electrode scale is possible H. Strehlow, W. Knoche, H. Schneider, Ber. Bunsenges. Phys. Chem. 77 (1973) 760;
(b) G. Gritzner, J. Kuta, Pure Appl. Chem. 56 (1984) 461.
[21] T. Stein, H. Lang, R. Holze, J. Electroanal. Chem. 520 (2002) 163.
[22] G.D. Broadhead, J.M. Osgerby, P.L. Pauson, J. Chem. Soc. (1958) 650.
[23] K.L. Rinehart Jr., R.J. Curby Jr., P.E. Sokol, J. Am. Chem. Soc. 79 (1957) 3420.
[24] H. Lang, D. Seyferth, Z. Naturforsch. B 45 (1990) 212.
[25] W. Frosch, S. Back, H. Lang, J. Organomet. Chem. 621 (2001) 143.
[26] (a) T. Kottke, D. Stalke, J. Appl. Crystallogr. 26 (1993) 615;
(b) T. Kottke, R.J. Lagow, D. Stalke, J. Appl. Crystallogr. 29 (1996) 465;
(c) D. Stalke, Chem. Soc. Rev. 27 (1998) 171.
[27] G.M. Sheldrick, Acta Crystallogr., Sect. A 46 (1990) 467.
[28] G.M. Sheldrick, SHELXL-97: Program for Crystal Structure Refinement, University of Göttingen, Göttingen, Germany, 1997.
[29] A.L. Spek, PLATON-94 (V-101094): A Multipurpose Crystallographic Tool, University of Utrecht, Utrecht, The Netherlands, 1994.